Martian Atmospheric Modeling of Scale Factors for MarsGRAM 2005 and the MAVEN Project

Chris McCullough
Mentor: Allen Halsell

Summer 2011

Contents

List of Figures

INTRODUCTION/OBJECTIVE

For spacecraft missions to Mars, especially the navigation of Martian orbiters and landers, an extensive knowledge of the Martian atmosphere is extremely important. The generally-accepted NASA standard for modeling of the Martian atmosphere is called the Mars Global Reference Atmospheric Model (MarsGRAM), which was developed at Marshall Space Flight Center. MarsGRAM is useful for tasks such as aerobraking, performance analysis and operations planning for aerobraking, entry descent and landing, and aerocapture [2]. Unfortunately, the densities for the Martian atmosphere in MarsGRAM are based on table look-up and not on an analytical algorithm. Also, these values can vary drastically from the densities actually experienced by the spacecraft. This does not have much of an impact on simple integrations but drastically affects its usefulness in other applications, especially those in navigation. For example, the navigation team for the Mars Atmosphere Volatile Environment (MAVEN) Project uses MarsGRAM to target the desired atmospheric density for the orbiter's periapse passage, its closest approach to the planet. After the satellite's passage through periapsis the computed density is compared to the MarsGRAM model and a scale factor is assigned to the model to account for the difference [3]. Therefore, large variations in the atmosphere from the model can cause unexpected deviations from the spacecraft's planned trajectory. In order to account for this, an analytical stochastic model of the scale factor's behavior is desired. The development of this model will allow for the MAVEN navigation team to determine the probability of various Martian atmospheric variations and their effects on the spacecraft.

APPROACH

To begin the creation of the probabilistic model of the scale factors used to model the Martian atmosphere, data from past and current Mars missions is required. The data used for this analysis is composed of data acquired from Mars Global Surveyor (MGS), Odyssey, and Mars Reconnaissance Orbiter (MRO). In addition, Brain Young has created a simplistic model of the scale factors, using only MRO data, which takes into account the scale factor variations with time during MRO's mission. These variations, shown in figure 1, exhibit a random behavior over the lifetime of MRO [7].

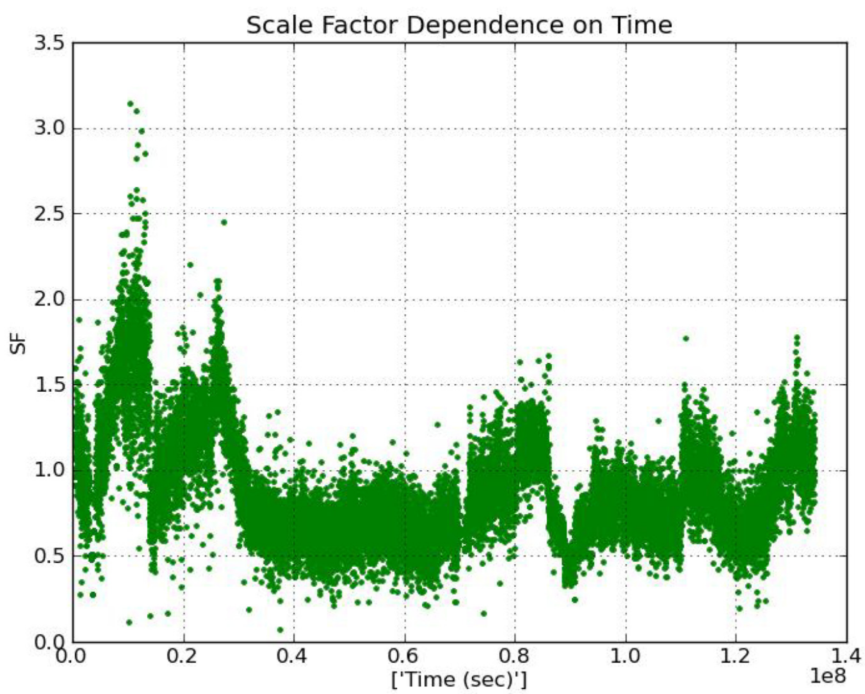

Figure 1: MRO Scale Factor for Mission Duration [7]

In an attempt to recreate this, Brian Young, developed a statistical model that simply places random noise about a mean scale factor of 1. This model is given by equation 1.

$$sig(x) = tanh^2(\sqrt{x})$$

$$l_t = \overline{l_t} + N(0, \sigma_0)$$

$$\overline{l_{t+n}} = \overline{l_t} e^{-\alpha\lambda n} + N(0, \sigma_0 \sqrt{\frac{\alpha}{2\lambda} sig(2\alpha\lambda n)} \tag{1}$$

$$l_{t+n} = \overline{l_t} e^{-\alpha\lambda n} + N(0, \sigma_0 \sqrt{1 + \frac{\alpha}{2\lambda} sig(2\alpha\lambda n)}$$

$$SF_{t+n} = e^{l_{t+n}}$$

In equation 1, sig is the sigmoid function, SF_{t+n} is the scale factor at time t plus n orbit revolutions, l_{t+n} is the scale factor's logarithmic equivalent, and $\overline{l_{t+n}}$ is the mean of the scale factor's logarithmic equivalent. Also, σ_0, α, and λ are the base noise, averaging coefficient, and decay rate respectively. These values are shown in table 1.

Table 1: Values for Base Noise, Averaging Coefficient, and Decay Rate

$Coefficient$	$Value$
σ_0	0.1183165
α	0.00998
λ	0.17528

Using this model as a baseline [7], dependence of the scale factor on other parameters can be examined. Once these relationships have been plotted and examined, they can be fit to an analytical equation. This fit of the data will be the mean value in the probabilistic model.

RESULTS/DISCUSSION

SCALE FACTOR CREATION

The first point of emphasis in the data analysis involved the reconstruction of the scale factors. For MRO this was not a problem since the data sets were relatively new and already contained scale factors determined from the orbit determination process. However, with MGS and Odyssey, only density values were available from the orbit determination process. Therefore, these had to be converted into the desired scale factors. This process was done by examining the inputs into MarsGRAM 2005 for MRO, and using a very simple iterative optimization to acquire the best possible scale factor estimates for MGS and Odyssey. Once this process was completed the scale factors for each of the missions was available for further analysis. This scale factors for each mission over their mission duration are shown in figure 2.

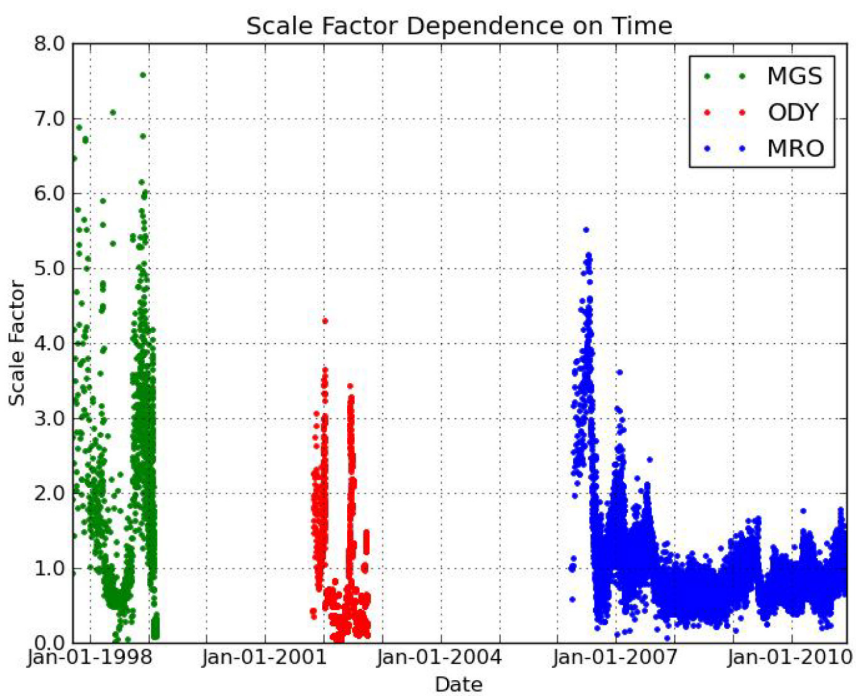

Figure 2: Scale Factors for MGS, Odyssey, and MRO

SCALE FACTOR DEPENDENCE ON STATE PARAMETERS

To begin the data analysis, a variety of factors needed to be examined to determine if the scale factor values had any dependence on the spacecraft's state. Some of the state values that were examined are altitude, latitude, longitude, mean local solar time, and the Martian season.

The Martian seasons seem to play a small role in the evolution of the Martian atmosphere, as well as in the scale factor values for spacecraft missions. The Martian seasons cause much larger temperature, and therefore atmospheric fluctuations than the seasons of Earth. This is due to two main factors: the eccentricity of the Martian orbit and the lack of a global magnetic field. First the eccentricity of the Martian orbit is 0.094. Compared to the Earth's eccentricity, which is 0.017, this is rather high. In fact, behind Pluto and Mercury, Mars has the 3rd highest eccentric orbit [6]. This eccentricity causes Mars to vary in distance from the Sun, amplifying the affect to the seasons. Also, since Mars does not have a global magnetic field there is nothing to shield the Martian atmosphere from solar radiation. Therefore, the Sun's rays affect the atmosphere differently during each season. Using seasonal information acquired from the Planetary Society [4], the scale factors can be plotted according to season. This plot is shown in figure 3.

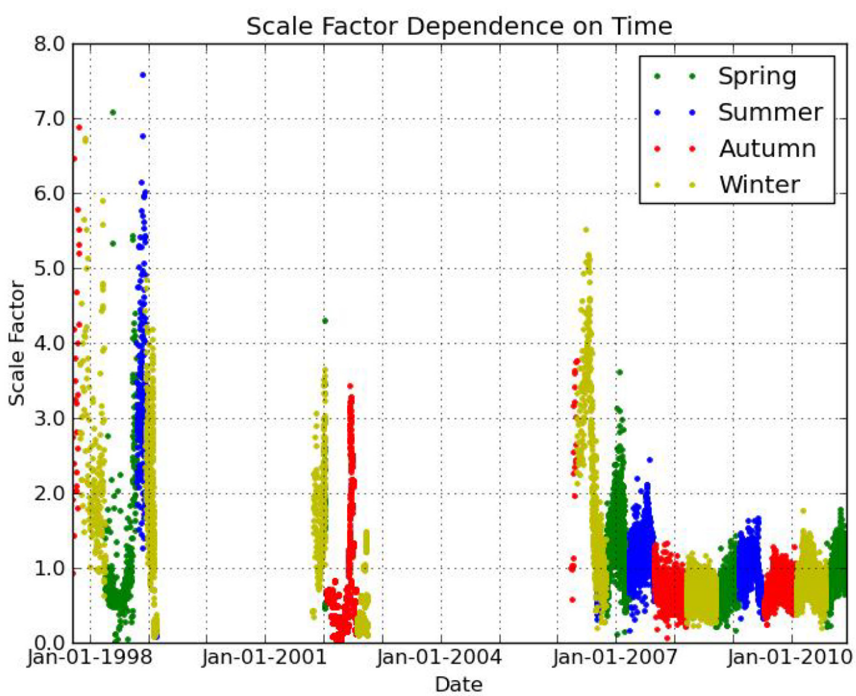

Figure 3: Scale Factor Dependence on Season

From figure 3, we can see a slight oscillation due to the seasonal affects on Mars. This is most noticeable on the right side of the plot (MRO's Science Phase), as the scale factor seems to peak during the summer and then fall back down during autumn and winter.

The mean local solar time and the longitude are other parameters that were examined for possible scale factor dependence. The mean local solar time is the "effective" time of the day on Mars. For example, if the Martian day were 24 "hours" long, an hour on Mars would be slightly longer than an hour on Earth. This is due to the slower spin rate of Mars. This is an important factor to analyze because it effectively measures the scale factor dependence on whether it is day or night on Mars. The plots for local mean solar time and longitude are shown in figure 4.

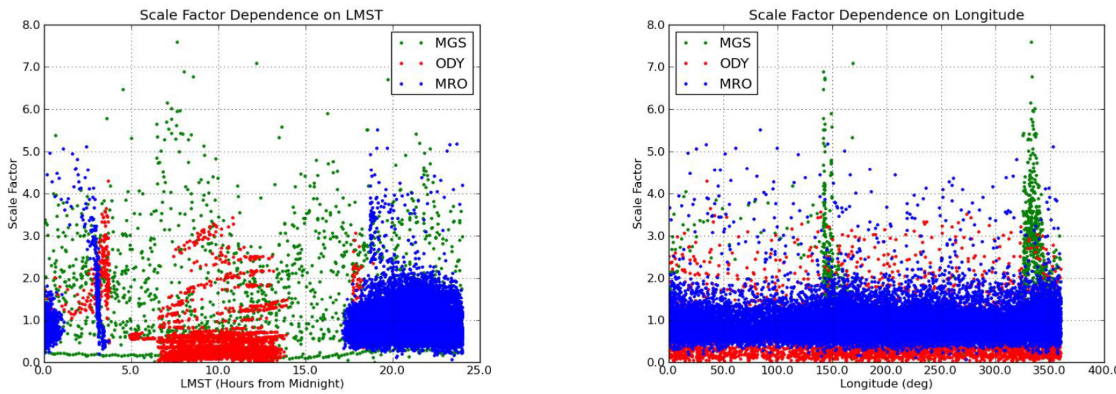

(a) (b)

Figure 4: Scale Factor Dependence on Mean Local Solar Time (a) and Longitude (b)

From figure 4, we can see that neither the mean local solar time nor longitude, have a drastic affect on the atmospheric scale factors. However, in the plot vs. longitude we can see a slight sine wave near the top of the scatter. This is expected and due to density waves, which can be modeled in MarsGRAM 2005. However, since MarsGRAM 2005 can model these, they are time dependent, a small effect, and vary greatly there will be no attempt to model them.

Another factor that was expected to affect the atmospheric scale factor is the altitude of the satellite. It was expected that at lower altitudes the scale factor might trend to be much higher than that at higher altitudes. Figure 5 shows the scale factor dependence on altitude.

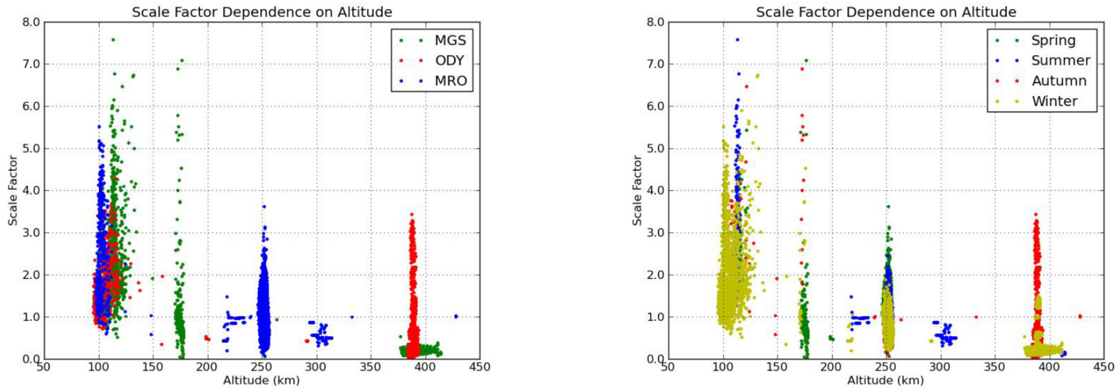

(a) (b)

Figure 5: Scale Factor Dependence on Altitude with Color Coding According to Spacecraft (a) and Season (b)

From figure 5, we can see that the data is quite limited. There are only discrete pockets of altitude instead of a continuous altitude distribution that would allow for the fitting of a trend. Also, there appears to be not much of difference in the distribution over various altitudes, therefore, the altitude will not factor in to the model either.

Finally, the dependence of the scale factor on the satellite's latitude must be examined. This plot is shown in figure 6.

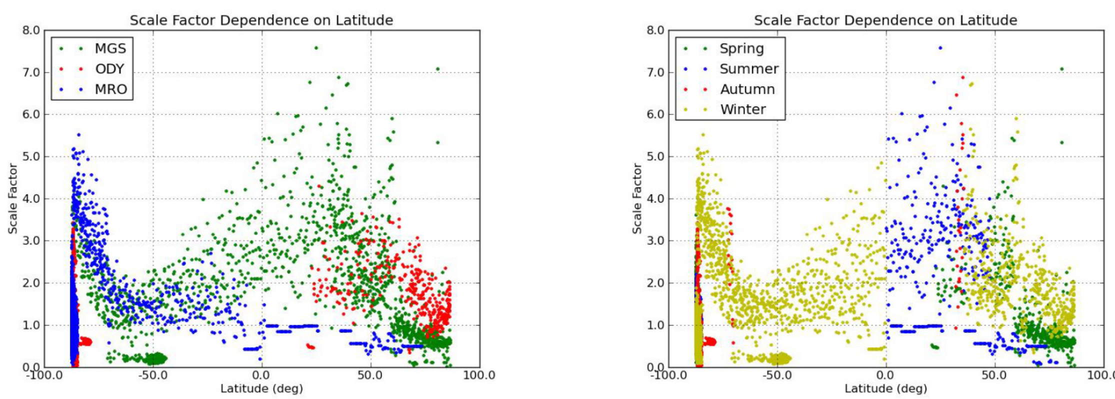

(a) (b)

Figure 6: Scale Factor Dependence on Latitude with Color Coding According to Spacecraft (a) and Season (b)

From this figure, there is definitely a trend in the atmospheric scale factor according to latitude. On the left side of the plot there appears to be a large spike in the scale factor, but upon further scrutiny there is also a dense region where the scale factor is low as well. The differences here are due to two different types of data being present. The spike is due to the data acquired from the aerobraking phase of the missions, while the dense area that is closer to a scale factor of one is from the science phase of the missions. The other spike in the data set occurs near latitude of approximately 30 degrees north. This could possibly be due to the topography of Mars. Upon examining a topographical map of Mars, shown in figure 7, we see that the spikes correspond to large shifts in the Martian topography. If a topographical map for Mars is examined, it is obvious that at this latitude the height of the Martian surface drops dramatically.

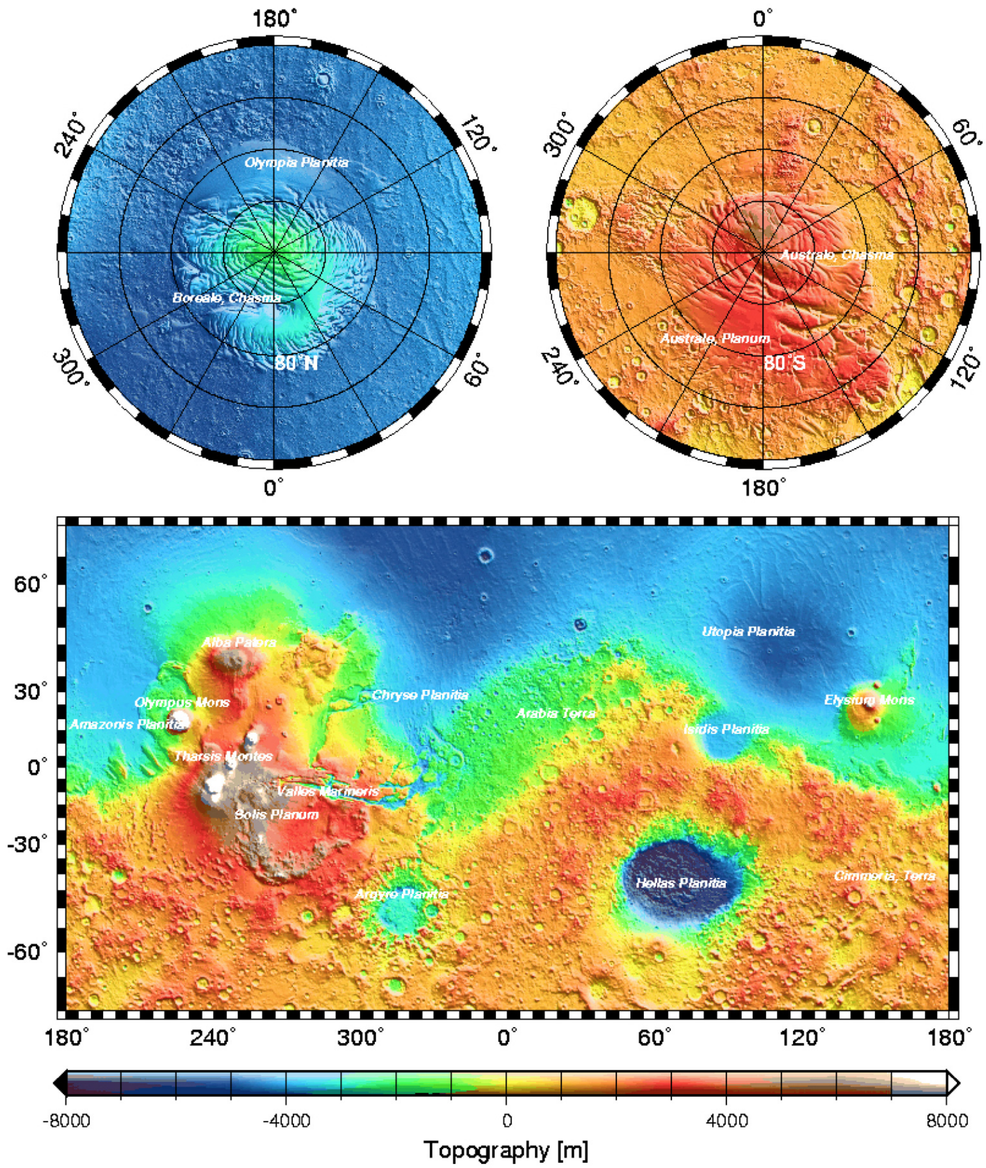

Figure 7: Martian Topography Map [5]

From figure 7 we can see that the spikes in the scale factor at latitudes near the south pole and at approximately 30° correspond to large increases and decreases, respectively, in the Martian surface elevation. Therefore, the surface elevation could be a determining factor in the MarsGRAM 2005 modeling error.

MATHEMATICAL MODELING OF THE SCALE FACTORS

From the figures above, it is apparent that the scale factor has a dependence on the Martian season and the spacecraft's latitude. These exact dependencies must be determined to create the mathematical model. This will be done by doing a least squares fit of a polynomial, for the latitude dependence, and a sine wave, for the seasonal dependence, to the data shown above. Also, the deviation statistics of the scale factor model will utilize the parameters σ_0, α, and λ from equation 1 and table 1. This fit will be done for two separate cases. First, the fit will be done using the entire data set shown in the previous figures. Second, the fit will be recreated for the data set without the MRO and Odyssey science data. This second fit will eliminate the large block of data at the southern latitudes in figure 6, allowing the least squares fit to follow the upward trend in scale factors.

MODEL USING FULL DATASET

For the full dataset, the seasonal variations were fit using a sine wave, while the latitudinal variations were fit with a fifth order polynomial. The equations for the probabilistic model are shown in equation 2.

$$
\begin{aligned}
sig(x) &= tanh^2(\sqrt{x}) \\
l_t &= \overline{l_t} + N(0, \sigma_0) \\
\overline{l_{t+n}} &= \overline{l_t} e^{-\alpha\lambda n} + N(0, \sigma_0 \sqrt{\frac{\alpha}{2\lambda} sig(2\alpha\lambda n)}) \\
l_{t+n} &= \overline{l_t} e^{-\alpha\lambda n} + N(0, \sigma_0 \sqrt{1 + \frac{\alpha}{2\lambda} sig(2\alpha\lambda n)}) \\
\beta_{t+n} &= l_{t+n} + \nu_0 + \nu_1(lat) + \nu_2(lat)^2 + \nu_3(lat)^3 + \nu_4(lat)^4 + \nu_5(lat)^5 \\
&\quad + A(lat) sin(f(JD) + \theta) \\
SF_{t+n} &= e^{\beta_{t+n}}
\end{aligned}
\tag{2}
$$

In equation 2, the parameters are the same as in equation 1 except for the introduction of β as the logarithmic scale factor equivalent. Also, the fit parameters are given by ν, A, f, and θ. The fit parameters are given in table 2.

Table 2: Values for Full Dataset Fit Parameters

$Coefficient$	$Value$
ν_0	0.5315
ν_1	0.01928
ν_2	$-9.73e-5$
ν_3	$-6.397e-6$
ν_4	$-5.7717e-10$
ν_5	$5.1290e-10$
A	-0.00373
f	0.008882963
θ	3235881.98

From the fit parameters in table 2, we can view the trend lines with the dataset to see how well they match the data. These are shown in figure 8.

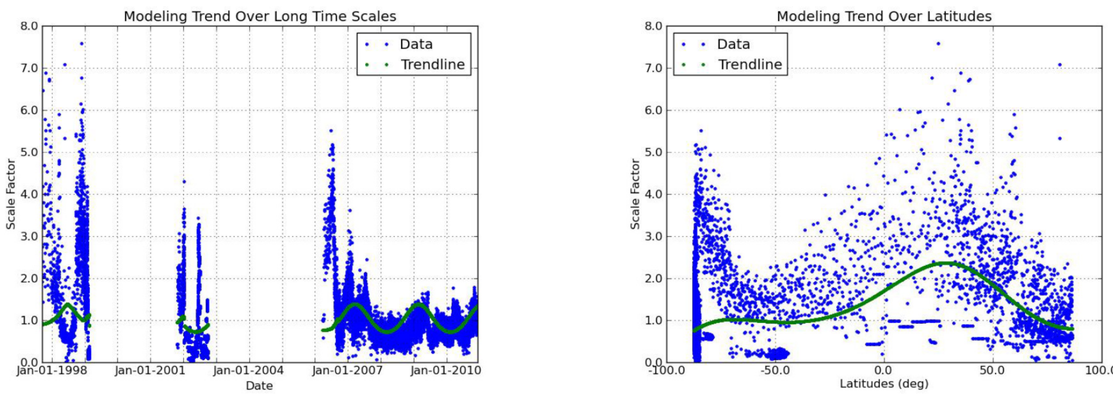

(a)

(b)

Figure 8: Trend Lines for Fit of Full Dataset with Time (a) and Latitude (b)

From figure 8, we can see that the fit matches the data quite well; however, in figure (b) the large block of science data at the south pole skews the fit at the south pole towards one. This could be a desired effect if the spacecraft we are attempting to model has similar characteristics to the orbits of the science data phases, mainly a circular orbit. Now, if we plot the full model, which is shown in equation 2, we can see how well the model matches the true data. These figures are shown in figure 9.

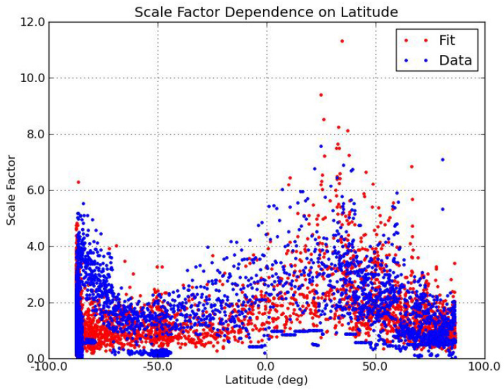

(a)

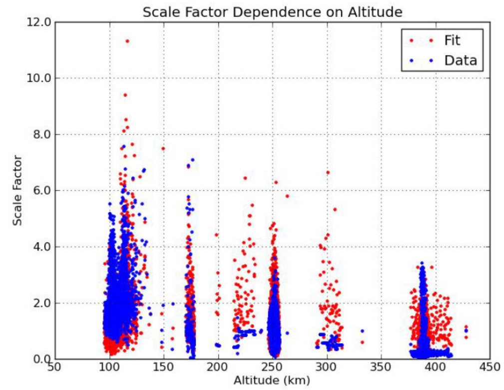

(b)

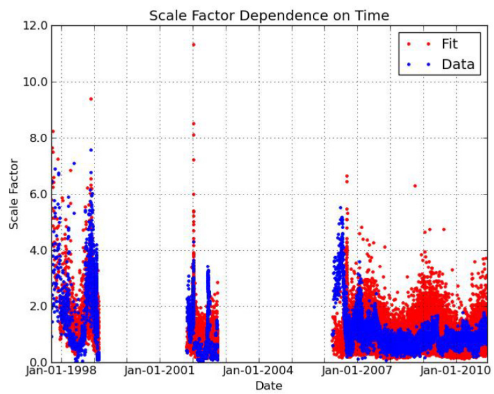

(c)

Figure 9: Scale Factor Fits for Full Dataset with Dependence on Latitude (a), Altitude (b), and Date (c)

From figure 9, we can see that the fit matches quite well with the real data. The only, pitfall appears to be in the deviation fit; however, the deviation overestimates the variability of the scale factors. This yields a conservative estimate that could account for any other errors or deviations.

MODEL USING AEROBRAKING DATASET

The aerobraking dataset differs from the full dataset in that the science data for MRO and Odyssey has been removed to eliminate the large strip of data at low latitudes. This leaves only the highly elliptical data from the aerobraking and transition phases of all the missions. For this fit the seasonal variations were not fit to a sine wave, as the full dataset was, while the latitudinal variations were fit with a sixth order polynomial. The seasonal variations were left out because the elimination of the MRO science data removes most of the noticeable seasonal trends. Therefore, the seasonal fit would not provide a reliable fit and should be thrown out. However, if a seasonal fit is desired the sine wave determined in the fit of the full dataset can be used in conjunction with the following fit. The equations for the probabilistic model are shown in equation 3.

$$
\begin{aligned}
sig(x) &= tanh^2(\sqrt{x}) \\
l_t &= \overline{l_t} + N(0, \sigma_0) \\
\overline{l_{t+n}} &= \overline{l_t} e^{-\alpha\lambda n} + N(0, \sigma_0 \sqrt{\frac{\alpha}{2\lambda} sig(2\alpha\lambda n)} \\
l_{t+n} &= \overline{l_t} e^{-\alpha\lambda n} + N(0, \sigma_0 \sqrt{1 + \frac{\alpha}{2\lambda} sig(2\alpha\lambda n)} \\
\beta_{t+n} &= l_{t+n} + \nu_0 + \nu_1(lat) + \nu_2(lat)^2 + \nu_3(lat)^3 + \nu_4(lat)^4 + \nu_5(lat)^5 + \nu_6(lat)^6 \\
SF_{t+n} &= e^{\beta_{t+n}}
\end{aligned}
\tag{3}
$$

In equation 3, the parameters are the same as in equation 1 except for the introduction of β as the logarithmic scale factor equivalent. Also, the fit parameters are given by ν. The fit parameters are given in table 3.

Table 3: Values for Aerobraking Fit Parameters

$Coefficient$	$Value$
ν_0	0.5422
ν_1	0.02956
ν_2	$-9.583e-5$
ν_3	$-9.7756e-6$
ν_4	$1.0437e-11$
ν_5	$6.0063e-10$
ν_6	$1.8850e-12$

From the fit parameters in table 3, we can view the trend lines with the dataset to see how well they match the data. These are shown in figure 10.

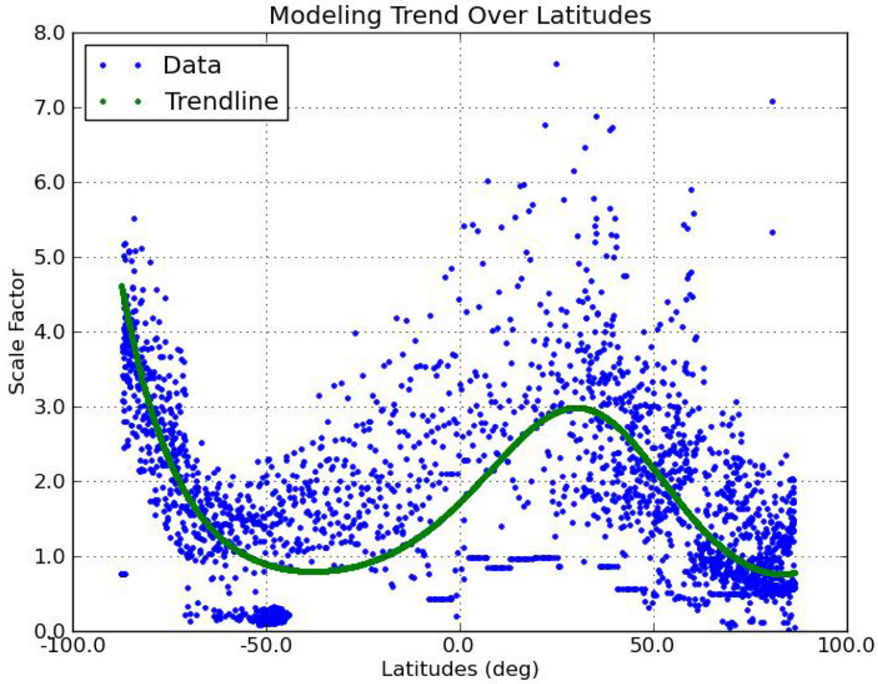

Figure 10: Trend Line for Fit of Aerobraking Dataset with Latitude

From figure 10, we can see that the fit matches the data quite well, especially in the southern regions where the trend now follows the upward spike. Now, if we plot the full model, which is shown in equation 3, we can see how well the model matches the true data. These figures are shown in figure 11.

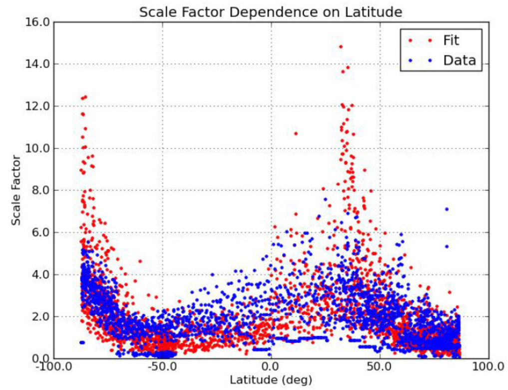

(a)

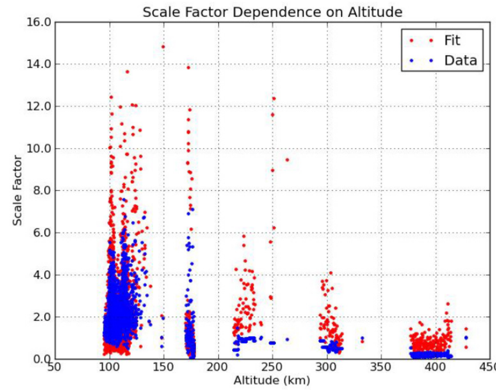

(b)

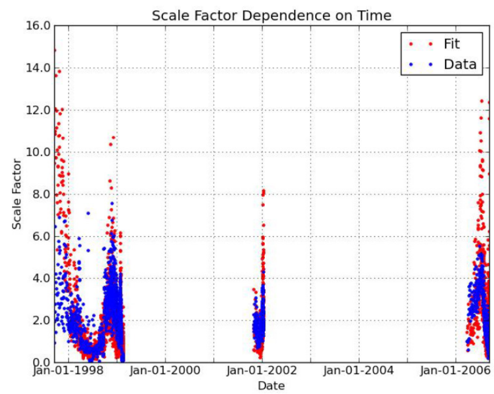

(c)

Figure 11: Scale Factor Fits for Aerobraking Dataset with Dependence on Latitude (a), Altitude (b), and Date (c)

From figure 11, we can see that the fit matches quite well with the real data. However, just like in the full dataset the only pitfall appears to be in the deviation fit. Just as in the case of the full dataset, the deviation overestimates the variability of the scale factors, yielding a conservative estimate that could account for any other errors or unexpected deviations.

MODEL LIMITATIONS

Although this model appears to fit the data quite well, there are some limitations that should be known when using this model. First, the model is created from a limited data set. It only involves three missions: MGS, Odyssey, and MRO; which have distinct orbital characteristics. For example, when viewing the plots that show altitude dependence we can see that the altitudes are only at distinct steps, instead of a continuous distribution. This limits the effectiveness of the model at other altitudes. In addition, if a satellite is in an orbit that is not similar to the orbits of MGS, Odyssey, and MRO the model might not model them effectively. Also, this model was developed from some scale factors that had to be explicitly created. Therefore, any error in the creation of these scale factors, such as in modeling the Martian dust storms, and creating the inputs to MarsGRAM 2005 could skew the model. Finally, for this model all of the data was weighted equally, meaning that if there are some poor quality measurements in the datasets they could affect the validity of the fit.

CONCLUSIONS AND FUTURE WORK

From the examination of these three extensive Mars missions, it is apparent just how variable the Martian atmosphere is. Due to its lack of a global magnetic field, the solar fluctuations and seasonal variance of the Martian orbit drastically affect the stability of the Martian atmosphere, making it difficult to predict and plan for a Martian spacecraft. This also makes a probabilistic model of the atmospheric scale factor such a valuable commodity. Any improved accuracy in the Martian atmospheric modeling correlates to an improved accuracy in spacecraft navigation and prediction of spacecraft trajectories. In examining MarsGRAM 2005, there is an obvious dependence on the spacecraft's state with the accuracy of the MarsGRAM model. In the mathematical models developed above there is a definite dependence on the Martian season and the latitude of the spacecraft. In addition to this there could be some correlation with the spacecraft's altitude; however, there is not enough data at various altitudes to support this claim. This could be an area of focus for further study of MarsGRAM as more data becomes available from future missions. Also, MarsGRAM 2010 has recently been released and could possibly show different characteristics from the results shown above. Further examination of this new model and its modeling errors could be another area of emphasis for further studies.

REFERENCES

[1] *Goddard Space Flight Center*. **The Mars Orbiter Laser Altimeter Image Gallery**. 25 July, 2011. http://mola.gsfc.nasa.gov/images.html

[2] Justus, C. G. **Mars Global Reference Atmospheric Model 2010**. *National Aeronautics and Space Administration*. 12 June, 2011. see.msfc.nasa.gov/tte/model_Marsgram.htm

[3] MAVEN Navigation Team. MAVEN CDR (Critical Design Review)

[4] *Space Topics: Mars' Calendar*. **The Planetary Society**. 11 July, 2011. http://planetary.org/explore/topics/mars/calendar.html

[5] *Mars - The Cold Red Wilderness*. **Visions of the Cosmos**. 22 July, 2011. http://www.visionsofthecosmos.co.uk/Planet%20Mars.htm

[6] Williams, Dr. David R. *Planetary Fact Sheet*. 22 July, 2011. http://nssdc.gsfc.nasa.gov/planetary/factsheet/

[7] Young, Brian. *MarsGRAM2005 Scale Factor Monte Carlo Modeling for MAVEN Corridor Maintenance Studies*. 9 February, 2011.

ACKNOWLEDGEMENTS

This research was carried out at the Jet Propulsion Laboratory, California Institute of Technology, and was sponsored by the National Space Grant College and Fellowship Project and the National Aeronautics and Space Administration. It is also in affiliation with the University of Texas at Austin and the Center for Space Research.

I would also like to acknowledge several people. I would like to thank my mentor Allen Halsell for giving me the opportunity to come to JPL for the summer and for his guidance and help during the summer. Also, I would like to thank my co-mentor, Stuart Demcak, and Brian Young for their assistance and guidance during my summer research.